Evaluation of Brain Pharmacokinetics (PK) and Tumor Growth Inhibition of PARP Inhibitors in Mouse Xenograft Models Using Semi-Mechanistic PK/Pharmacodynamic (PD) Modeling

Poster No. 3219

Michelle Liao,[1] Feng Jin,[2] Minh Nguyen,[1] Liliane Robillard,[1] Andrew D. Simmons,[1] Thomas C. Harding,[1] Jim J. Xiao[1]

[1]Clovis Oncology, Inc., Boulder, CO, USA; [2]Polaris Consulting, Inc., San Francisco, CA, USA

INTRODUCTION

- The poly(ADP-ribose) polymerase (PARP) inhibitors rucaparib, niraparib, and olaparib have shown antitumor activity against various types of cancer[1-3]; however, few studies have been conducted on their activity against intracranial tumors, and results have been inconclusive[4-8]
- We evaluated the brain penetration and the antitumor effects of selected PARP inhibitors in orthotopic and intracranial tumor mouse models
  - In vivo PK studies confirmed the limited brain penetration of PARP inhibitors evaluated in a murine model with an intact blood–brain barrier.[8,9] However, rucaparib and niraparib demonstrated antitumor activity in a *BRCA1*-mutant, intracranial, triple-negative breast cancer (TNBC) mouse model[9]
  - Clinical activity has also been observed in patients with germline *BRCA2*-mutant breast cancer and central nervous system (CNS) involvement treated with rucaparib or olaparib[9,10]
- Here, we developed a semi-physiologically based PK model to characterize plasma, brain, and cerebrospinal fluid (CSF) concentration–time profiles for various PARP inhibitors. Tumor growth inhibition (TGI) models were developed to characterize the PK/PD relationship between rucaparib or niraparib and tumor response data in intracranial tumor models

METHODS

PK Studies

- Plasma samples were collected from nontumor-bearing non-obese diabetic/severe combined immunodeficiency (NOD/SCID) female mice (n=3 mice/group) following a single oral dose of rucaparib at 2, 5, 15, 50, or 150 mg/kg
- Plasma, brain, and CSF samples were collected from male CD-1 mice (n=3 mice/group) following a single oral dose of rucaparib (150 mg/kg), niraparib (50 mg/kg), olaparib (150 mg/kg), or veliparib (150 mg/kg)[9]
- Total concentrations (bound + unbound) of each drug in plasma, brain homogenate, and CSF were determined using liquid chromatography-tandem mass spectrometry methods

Murine In Vivo Efficacy Studies

- Antitumor efficacy in MDA-MB-436 orthotopic model: MDA-MB-436 cells (TNBC cell line, *BRCA1* c.5396+1G>A) were implanted in the right mammary fat pad of NOD/SCID female mice; treatment with rucaparib (2, 5, 15, 50, or 150 mg/kg orally [PO] twice daily [BID] × 28 days) began at 200 mm^3 mean tumor size (n=10 mice/group)
- Intracranial efficacy: luciferase-expressing MDA-MB-436 cells were intracranially implanted in NOD/SCID female mice; treatment with rucaparib (150 mg/kg PO BID) or niraparib (50 mg/kg PO once daily [QD] × 57 days) started at mean bioluminescence imaging (BLI) signal of 2.4×10^7 photons/s (n=11–12 mice/group). BLI intensity is proportional to tumor size and was used as a surrogate for tumor size in the PK/PD modeling

Modeling Software

- A model was developed using NONMEM (version 7.3; ICON Development Solutions, Ellicott City, MD, USA) and R (version 3.5.1)

Figure 1. Model Development Process

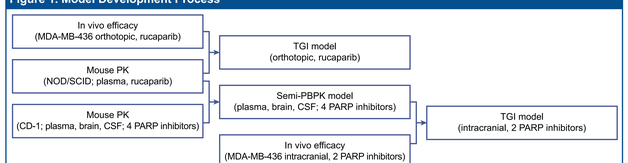

Four PARP inhibitors: rucaparib, niraparib, olaparib, and veliparib; 2 PARP inhibitors: rucaparib and niraparib.
CSF, cerebrospinal fluid; NOD/SCID, non-obese diabetic/severe combined immunodeficiency; PARP, poly(ADP-ribose) polymerase; PK, pharmacokinetics; PBPK, physiologically based pharmacokinetic; TGI, tumor growth inhibition.

RESULTS

PK Modeling of Rucaparib, Niraparib, Olaparib, and Veliparib

Figure 2. Model Structure[11] and Equations

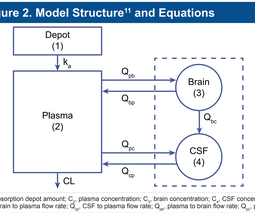

$$\frac{dA_1}{dt} = -k_a \times A_1$$

$$\frac{dC_2 \times V_p}{dt} = k_a \times A_1 - CL \times C_2 - Q_{pb} \times C_2 + Q_{bp} \times C_3 - Q_{pc} \times C_2 + Q_{cp} \times C_4$$

$$\frac{dC_3 \times V_b}{dt} = Q_{pb} \times C_2 - Q_{bp} \times C_3 - Q_{bc} \times C_3$$

$$\frac{dC_4 \times V_c}{dt} = Q_{pc} \times C_2 - Q_{cp} \times C_4 + Q_{bc} \times C_3$$

A_1, absorption depot amount; C_2, plasma concentration; C_3, brain concentration; C_4, CSF concentration; CL, clearance; CSF, cerebrospinal fluid; k_a, first-order rate absorption constant; Q_{bc}, brain to CSF flow rate; Q_{pb}, brain to plasma flow rate; Q_{bp}, CSF to plasma flow rate; Q_{pc}, plasma to brain flow rate; Q_{cp}, plasma to CSF flow rate; t, time; V_b, brain volume; V_c, CSF volume; V_p, plasma volume.

Model Assumptions

- The model equation was built on free concentration with plasma protein binding and brain tissue binding fixed on measured values.[9] Drug total concentrations in CSF were considered unbound
- Mouse weight = 20 g
- Mouse CSF volume = 0.0045 L/kg; fixed in model[12]
- Mouse brain volume = 0.018 L/kg; fixed in model[12]
- Data from all 3 compartments (plasma, brain, and CSF) were fitted simultaneously

Figure 3. Model-Fitted PARP Inhibitor Concentration Profiles: (A) Rucaparib; (B) Niraparib; (C) Olaparib; and (D) Veliparib

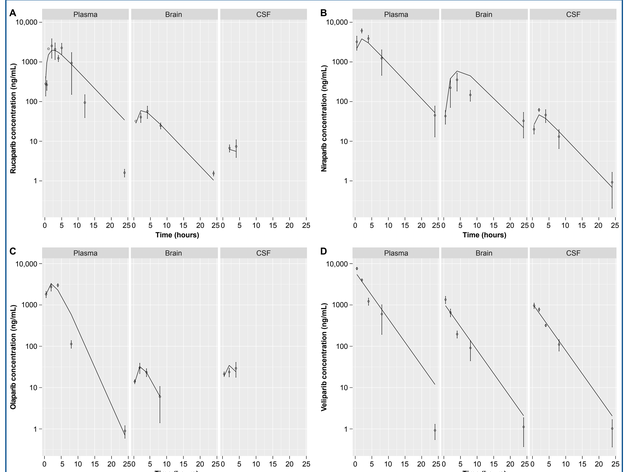

The circles denote the average observed drug concentration, the vertical lines indicate standard deviation, and the lines represent the model-fitted drug concentrations.
CSF, cerebrospinal fluid; PARP, poly(ADP-ribose) polymerase.

- Different model structures (eg, adding flow from CSF to brain) were tested. However, these attempts did not result in a statistically significant improvement in describing the data (P<0.05)

Table 1. Model-Estimated PK Parameters

Parameters	Units	Rucaparib	Niraparib	Olaparib	Veliparib
CL	L/h/kg	31.9	10.9	70.1	10.7
V_p	L/kg	12.6	8.81	13.2	24.4
Q_{pb}	L/h/kg	0.158	0.0100	0.00947	0.344
Q_{bp}	L/h/kg	12.3	0.0100	0.165	1.52
V_b (fixed)	L/kg	0.018	0.018	0.018	0.018
Q_{pc}	L/h/kg	0.059	0.183	2.15	0.608
Q_{cp}	L/h/kg	11.8	2.54	24.9	2.60
V_c (fixed)	L/kg	0.0045	0.0045	0.0045	0.0045
Q_{bc}	L/h/kg	9.06	0.0821	0.154	1.15
k_a	1/h	0.203	1.04	0.436	19.9
$f_{u,plasma}$ (fixed)[9]	-	0.296	0.165	0.119	0.593
$f_{u,brain}$ (fixed)[9]	-	0.0724	0.0819	0.367	0.438

CL, clearance; CSF, cerebral spinal fluid; $f_{u,plasma}$, free concentration with plasma protein binding; $f_{u,brain}$, free concentration with brain tissue binding; k_a, first-order rate absorption constant; PK, pharmacokinetic; Q_{bc}, brain to CSF flow rate; Q_{pb}, brain to plasma flow rate; Q_{bp}, CSF to plasma flow rate; Q_{pc}, plasma to brain flow rate; Q_{cp}, plasma to CSF flow rate; V_b, brain volume; V_c, CSF volume; V_p, plasma volume.

- Parameter uncertainties were not reportable (**Table 1**), potentially because of the complexity of the physiologically based model structure
- Clearance and central volume estimates were comparable to those calculated using noncompartmental analyses (data not shown)

TGI Model for Characterizing Antitumor Efficacy of Rucaparib in an Orthotopic Model

Figure 4. Model Structure[13]

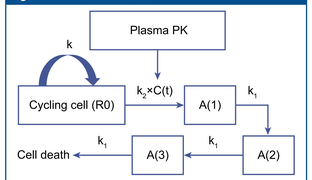

Tumor volume is the sum of R0, A(1), A(2), and A(3).
A(1), A(2), A(3), transit tumor compartments leading to cell death; C(t), drug concentration at time t; k, first-order growth rate; k_1, rate constant for tumor cell death; k_2, index of drug efficacy; PK, pharmacokinetics; R0, tumor volume when treatment starts.

Table 2. Model-Estimated PK/PD Parameters

Parameter	Estimates (RSE, %)
k	0.0566 (2.59)
R0	225 (2.92)
k_2	0.000497 (5.67)
k_1	0.111 (2.82)

k, first-order growth rate; k_1, rate constant for tumor cell death; k_2, index of drug efficacy; PD, pharmacodynamic; PK, pharmacokinetic; R0, tumor volume when treatment starts; RSE, relative standard error.

Figure 5. Model-Fitted Tumor Volume Profiles in an Orthotopic Model

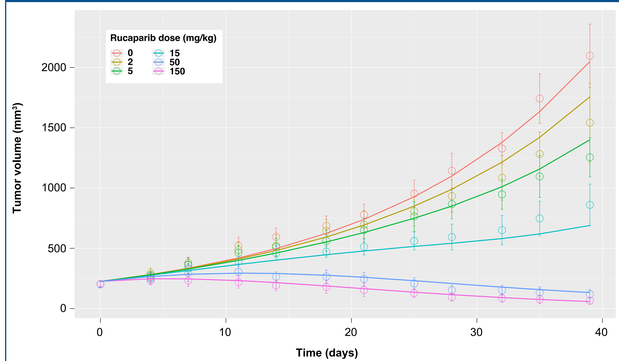

The circles denote the average observed tumor sizes; the vertical lines indicate standard deviation, and the lines represent the model-fitted tumor sizes.

- Although tumor growth inhibition models were tested (eg, dual zero- and first-order growth rate, Simeoni, transit-compartment model), they did not provide a statistically significant improvement in describing the data (P<0.05)
- Parameter uncertainty and relative standard error (RSE) were well estimated (**Table 2**)

TGI Model for Characterizing Antitumor Efficacy of Rucaparib and Niraparib in an Intracranial Model

Figure 6. Model Structure[13]

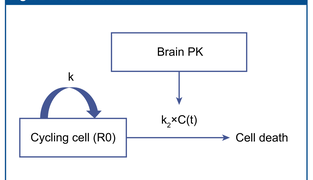

C(t), drug concentration at time t; k, first-order growth rate; k_2, index of drug efficacy; PK, pharmacokinetics; R0, tumor volume when treatment starts.

Table 3. Model-Estimated PK/PD Parameters

Parameter	Estimates (RSE, %)
k	0.146 (3.28)
R0	19.9 (10.2)
k_2, Rucaparib	0.0791 (2.16)
k_2, Niraparib	0.00891 (3.02)

k, first-order growth rate; k_2, index of drug efficacy; PD, pharmacodynamic; PK, pharmacokinetic; R0, tumor volume when treatment starts; RSE, relative standard error.

Figure 7. Model-Fitted Tumor Bioluminescence Profiles in an Intracranial Model

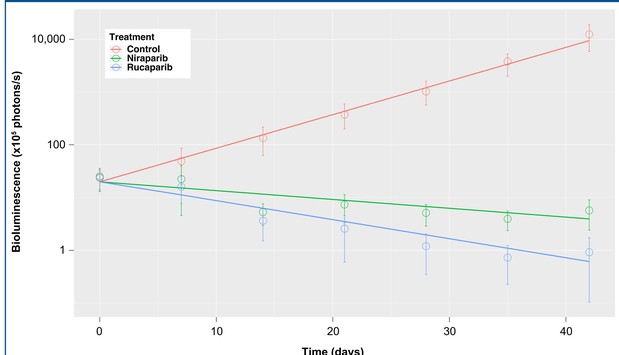

The circles denote the average observed tumor bioluminescence, the vertical lines indicate standard deviation, and the lines represent the model-fitted tumor bioluminescence.

- Although different tumor growth inhibition models were tested (eg, dual zero- and first-order growth rate, Simeoni model,[13] transit-compartment model), they did not provide statistically significant improvement in describing the data (P<0.05)
- Parameter uncertainty and RSE were well estimated (**Table 3**)

CONCLUSIONS

- **A semi-physiologically based PK model adequately characterized concentration profiles of 4 PARP inhibitors in plasma, brain, and CSF in mice**
- **Modified Simeoni model[13] adequately described tumor inhibition data collected in a murine orthotopic model (rucaparib) and in a murine intracranial efficacy model (rucaparib and niraparib)**
- **The mouse intracranial efficacy data are consistent to the previously reported clinical efficacy in a patient with *BRCA2*-mutant breast cancer and brain metastases[9]**

REFERENCES

1. Rubraca® (rucaparib) tablets [prescribing information]. Boulder, CO: Clovis Oncology, Inc.; 2020.
2. Zejula® (niraparib) capsules [prescribing information]. Research Triangle Park, NC: GlaxoSmithKline; 2020.
3. Lynparza® (olaparib) tablets [prescribing information]. Wilmington, DE: AstraZeneca Pharmaceuticals; 2020.
4. Karginova O et al. *Mol Cancer Ther*. 2015;14:920-30.
5. Sambade M et al. *Cancer Res*. 2018;78(13 suppl):abst 2813.
6. Kizilbash SH et al. *Mol Cancer Ther*. 2017;16:2735-46.
7. Murray J et al. *Br J Cancer*. 2014;110:1977-84.
8. Parrish KE et al. *Mol Cancer Ther*. 2015;14: 2735-43.
9. Nguyen M et al. *Cancer Res*. 2019;79(suppl):abst 3888.
10. Exman P et al. *NPJ Breast Cancer*. 2019;5:46.
11. Kielbasa W et al. *Drug Metab Dispos*. 2009;37:137–42.
12. Badhan RK et al. *Pharmaceutics*. 2014;6:97–136.
13. Simeoni M et al. *Cancer Res*. 2004;64:1094–101.

ACKNOWLEDGMENTS

This study was funded by Clovis Oncology, Inc. Medical writing and editorial support funded by Clovis Oncology, Inc., were provided by Stephen Mason and Frederique H. Evans of Ashfield Healthcare Communications.